Spatially Sparse Emitters Localization with QVBEM Algorithm

Esmaeil Ramezani

Email: e.ramez@chmail.ir
Department of Electrical Engineering, University of Isfahan.

ABSTRACT:
In this paper, we study the estimation of the spatially sparse radio emitter locations via the proposed Quad-tree variational Bayesian expectation maximization (QVBEM) algorithm. Firstly, we assume that the emitters are approximately lie on a uniform grid points in the region under surveillance. The VBEM algorithm is applied and the points exceeding the threshold level are considered as potential targets. Then, the grids are refined around the potential targets via the Quad-tree algorithm and the process is iterated. It allows us to find the location of sparse emitters with much less computational complexity due to the use of fewer grid points. Simulation results show the superiority of the QVBEM to existing methods. The impact of threshold value on the performance of QVBEM is also studied.

KEYWORDS: The author shall provide up to 10 keywords to help identify the major topics of the paper.

1. INTRODUCTION

Accurate localization of the co-channel emitters is important in some applications such as cognitive radio, wireless sensor network, and electronic warfare (EW) [1-2]. The focus of this work is on accurate localization of co-channel radars from the space. However, the proposed algorithm can be exploited to other applications. Since a few number of radars exist in a wide geographical area, we deal with a sparse localization problem. Localization is performed by two-dimensional direction of arrival (DoA) estimation. Many compressed sensing (CS) based methods have been proposed for sparse DoA estimation ([3] and references therein). Here, we propose the use of the combination of VBEM [4-6] and Quad-tree [7] techniques to achieve accurate radar localization in space borne EW receiver, which is called QVBEM. The computational load optimization of the QVBEM algorithm is investigated through suitable threshold selection in this work.

2. PROBLEM FORMULATION

Assume that an L-shape uniform linear array (ULA) of antennas is used for two-dimensional DoA estimation, according to Fig. 1. If M co-channel radars transmit their signals, the low-pass equivalent received signal at the origin of ULA, is given by (1).

$$u(t) = \sum_{i=1}^{M} s_i(t) e^{j2\pi f t} + \epsilon(t) \qquad (1)$$

where $s_i(t)$ is the baseband signal, transmitted by the i-th radar, and $\epsilon(t)$ denotes measurement noise and model mismatches. The received signal at each antenna element is filtered, down-converted and sampled, to form the measurement vector. Assume uniform grid points in the region under surveillance and a radar at point $p_i = (x_i, y_i)$, where its signal is received at EW receiver with azimuth and elevation DOAs, represented by φ_i and θ_i, respectively. The measurement vector at x-axis ULA can be written as (2).

$$\boldsymbol{g}_x^{(i)} = w_i \boldsymbol{\psi}_x^{(i)} + \boldsymbol{n}_x^{(i)} \qquad (2)$$

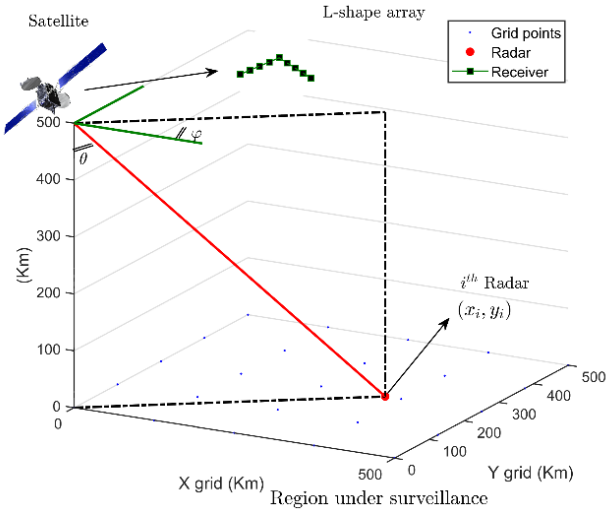

Fig. 1: Space-borne EW receiver, with the height 500Km from the earth, using an L-Shape uniform linear array for localization.

تاریخ دریافت: ۱۳۹۸/۰۹/۱۳ تاریخ پذیرش: ۱۳۹۸/۱۲/۰۱

In (2), $\boldsymbol{\psi}_x^{(i)}$ is steering vector , which is defined as below,

$$\boldsymbol{\psi}_x^{(i)} = \left[1, e^{j\phi_x^{(i)}}, e^{j2\phi_x^{(i)}}, \dots, e^{j(K-1)\phi_x^{(i)}}\right]^T \quad (3)$$

where $\phi_x^{(i)} = \frac{2\pi f d}{c}\frac{x_i}{r_i}$, K is the number of array element in each axis, d is the antenna elements spacing, r_i is the distance between the radar and the EW receiver, and c is the speed of light [2]. w_i is a value depends on the radar transmitting power, with $w_i \neq 0$ means that a radar really exists at point p_i.

By similar definition for y-axis ULA, we can write $\boldsymbol{g}_y^{(i)} = w_i\boldsymbol{\psi}_y^{(i)} + \boldsymbol{n}_y^{(i)}$. Finally, we can write $\boldsymbol{g}^{(p_i)} = w_i\boldsymbol{\psi}^{(p_i)} + \boldsymbol{n}^{(p_i)}$ where,

$$\begin{cases} \boldsymbol{\psi}^{(p_i)} = \left[\boldsymbol{\psi}_x^{(i)^T} \quad \boldsymbol{\psi}_y^{(i)^T}\right]^T \\ \boldsymbol{g}^{(p_i)} = \left[\boldsymbol{g}_x^{(i)^T} \quad \boldsymbol{g}_y^{(i)^T}\right]^T \\ \boldsymbol{n}^{(p_i)} = \left[\boldsymbol{n}_x^{(i)^T} \quad \boldsymbol{n}_y^{(i)^T}\right]^T \end{cases} \quad (4)$$

Note that in the definition of $\boldsymbol{\psi}_y^{(i)}$, we set $\phi_y^{(i)} = \frac{2\pi f d}{c}\frac{y_i}{r_i}$. Also, the common antenna between x-axis and y-axis, i.e. the element at the origin of L-shape array, only is considered in $\boldsymbol{\psi}_x^{(i)}$. Indeed, the first element of $\boldsymbol{\psi}_y^{(i)}$ is $e^{j\phi_y^{(i)}}$.

Assume that there are M radars, each one located at one of the possible grid points $p_1, p_2, \dots, p_N$ in the region under surveillance. By concatenating the vectors $\boldsymbol{g}^{(p_i)}$, $\boldsymbol{\psi}^{(p_i)}$ and $\boldsymbol{n}^{(p_i)}$ for $i = 1,2,\dots,N$, we finally have

$$\boldsymbol{g} = \Phi\boldsymbol{w} + \boldsymbol{n}, \quad (5)$$

where

$$\begin{cases} \boldsymbol{g} = [\boldsymbol{g}^{(p_1)} \quad \dots \quad \boldsymbol{g}^{(p_N)}] \\ \boldsymbol{n} = [\boldsymbol{n}^{(p_1)} \quad \dots \quad \boldsymbol{n}^{(p_N)}] \\ \Phi = [\boldsymbol{\psi}^{(p_1)} \quad \dots \quad \boldsymbol{\psi}^{(p_N)}] \end{cases} \quad (6)$$

and $\boldsymbol{w}$ is a $N \times 1$ vector with only M nonzero elements, corresponding to M radars. Since $M \ll N$, the vector $\boldsymbol{w}$ can be recovered from $\boldsymbol{g}$ using sparse recovery methods.

3. BAYESIAN RECOVERY METHODS AND VBEM

The Bayesian methods are usually used to approximate the posterior probability of the unknown variables. Assume that in (5), $\boldsymbol{n} \sim \mathcal{N}(.|\boldsymbol{0}, \sigma^2 I)$ where $\mathcal{N}(.|\boldsymbol{\mu}, \boldsymbol{\Sigma})$ denotes Gaussian distribution with mean $\boldsymbol{\mu}$ and covariance matrix $\boldsymbol{\Sigma}$. We can write:

$$p(\boldsymbol{g}|\boldsymbol{w}, \sigma^2) = (2\pi\sigma^2)^{-\frac{K}{2}} exp\left(-\frac{1}{2\sigma^2}\|\boldsymbol{g} - \boldsymbol{\Phi w}\|_2^2\right) \quad (7)$$

Let $\boldsymbol{w} = [w_1 \quad \dots \quad w_N]^T$, $\boldsymbol{\alpha} = [\alpha_1 \quad \dots \quad \alpha_N]$, $\beta = \frac{1}{\sigma^2}$. In [4] it is shown that by using hierarchical prior density functions given in (8),

$$\begin{cases} p(\boldsymbol{w}) = \prod_{i=1}^{N} \mathcal{N}(w_i|0, \alpha_i^{-1}) \\ p(\boldsymbol{\alpha}) = \prod_{i=1}^{N} \Gamma(\alpha_i|a, b) \\ p(\beta) = \Gamma(\beta|c, d) \end{cases} \quad (8)$$

the posterior density function $p(\boldsymbol{w}|\boldsymbol{g}, \boldsymbol{\alpha}, \sigma^2)$ is a multivariate Gaussian distribution with the mean vector $\boldsymbol{\mu}$ and covariance matrix $\boldsymbol{\Sigma}$, given by (9).

$$\begin{aligned} \boldsymbol{\Sigma} &= (\sigma^{-2}\boldsymbol{\Phi}^T\boldsymbol{\Phi} + \mathbf{A})^{-1} \\ \boldsymbol{\mu} &= \sigma^{-2}\boldsymbol{\Sigma}\boldsymbol{\Phi}^T\boldsymbol{g} \end{aligned} \quad (9)$$

where $\mathbf{A} = \text{diag}(\boldsymbol{\alpha})$, and $\Gamma(.|a, b)$ is the Gamma distribution function with shape parameter a and scale parameter b. The MAP estimation of $(\boldsymbol{\alpha}, \sigma^2)$ can be updated from measured data, $\boldsymbol{g}$, by maximizing $p(\boldsymbol{\alpha}, \sigma^2|\boldsymbol{g})$. The parameters $\boldsymbol{\Sigma}$, $\boldsymbol{\mu}$, $\boldsymbol{\alpha}$ and σ^2, can be iteratively updated from each other according to (9) and (10) [6].

$$\begin{cases} \alpha_i^{new} = \dfrac{1 - \alpha_i\boldsymbol{\Sigma}_{ii} + 2a}{\mu_i^2 + 2b} \\ (\sigma^2)^{new} = \dfrac{\|\boldsymbol{g} - \boldsymbol{\Phi\mu}\|_2^2 + 2d}{K - \sum_{i=1}^{N}(1 - \alpha_i\boldsymbol{\Sigma}_{ii}) + 2c} \end{cases} \quad (10)$$

After convergence, the MAP estimation of $\boldsymbol{w}$ is represented by $\boldsymbol{\mu}$.

The proper choice of parameters $a, b, c,$ and d is essential to have a good estimation. The idea behind variational Bayesian expectation maximization (VBEM) algorithm is adaptively changing these parameters, to introduce nonstationary Gaussian prior for capturing local characteristics of signal. In the VBEM algorithm, the hyper-prior distributions are assumed as $p(\boldsymbol{\alpha}) = \prod_{i=1}^{N}\Gamma(\alpha_i|\tilde{a}_i, \tilde{b}_i)$ and $p(\beta) = \Gamma(\beta|\tilde{c}, \tilde{d})$, where

$$\begin{cases} \tilde{a} = a + \dfrac{1}{2} \\ \tilde{b}_i = b + \dfrac{1}{2}\mathbf{E}^2[w_i] \\ \tilde{c} = c + \dfrac{K}{2} \\ \tilde{d} = d + \dfrac{1}{2}\mathbf{E}[\|\boldsymbol{g} - \boldsymbol{\Phi w}\|_2^2] \end{cases} \quad (11)$$

After convergence of VBEM, each w_i with the magnitude greater than a predefined threshold, can be considered as a target at location p_i. To improve the localization accuracy, the number of grid points must be increased. The computational complexity of the VBEM algorithm is $O(N^3)$ and it grows exponentially with N [2]. To resolve this problem, we propose to employ Quadtree algorithm in combination with VBEM.

4. QUAD-TREE+VBEM ALGORITHM

A Quad-tree is a tree data structure which is usually used for partitioning a two-dimensional image, through

subdividing it into four quadrants or regions [7]. We call the combination of the Quad-tree and the VBEM by QVBEM. At the first level of QVBEM algorithm, low-density grid points are assumed and the VBEM is used to estimate $\boldsymbol{w}$. The VBEM assumes that radars lie exactly on grid points, which is not practical assumption. To address this issue, we use the Quad-tree technique to refine the grid points around the potential radar locations and apply the VBEM again. To this end, each elements of $\boldsymbol{w}$, is evaluated and if its magnitude exceeds a predefined threshold, e.g. δ, is considered as a potential radar. At next levels of QVBEM, each potential target, which is associated with a grid point, is considered and refined grids with a half distance with respect to the previous level, is assumed around it. The matrix Φ is updated using these new grid points, according to (6), and the VBEM algorithm is run again. This process is iterated until the requited localization accuracy is achieved, or the available time for processing is expired. Fig. 2, shows the diagram of QVBEM.

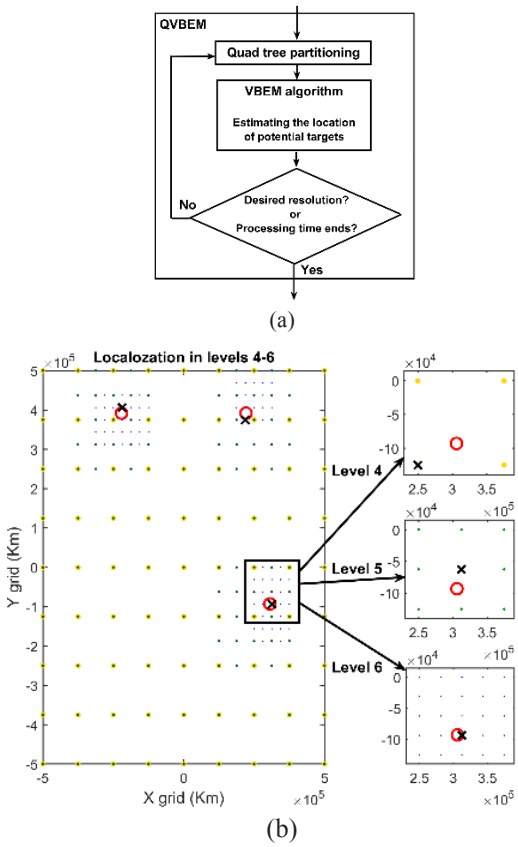

Fig. 2. (a) Block diagram of QVBEM (b) gridding refinement with Quad-tree technique in levels 4,5, and 6. × denotes the estimated location and ○ denotes the true location.

5. THRESHOLD SELECTION

Because of limited number of grid points, the radars do not lie exactly on the grids. Selecting p_i as location of a potential target at one level of the QVBEM algorithm, i.e. $|w_i| > \delta$, means that with high probability, there is a radar with location close to p_i. In such a condition, for the point p_j close to p_i, the value of $|w_j|$ may also be significant and the true target may be closer to p_j than p_i. Selecting a large δ may result in poor localization performance or even missing a target. On the other hand, an small δ leads to higher complexity, due to the more grid points in the next levels. Hence, there is a trade-off between localization accuracy and complexity in QVBEM method.

6. SIMULATION

$M = 3$ radars are considered in a $1000Km \times 1000Km$ region with random locations. The space-borne platform is assumed to be at the centre of the region under surveillance with the height $500Km$ (see Fig. 1) and the transmitted power of radars is considered in the order of 100 KWatt, which is transmitting power of a typical actual long range radar [8]. The radars carrier frequency is randomly selected in range $3 - 12GHz$ and the bandwidth is $50MHz$. The SNR is set to $15dB$. $K = 9$ antenna elements in a 2D L-shape ULAs are considered, where 5 antennas assumed in each axis.

Fig. 3-a shows the result of QVBEM localization after 8 levels of Quad-tree refinement. We set $\delta = 10$ and start with 4 grids at first level. At the 8-th level, the total number of grid points (i.e. the cumulative number of points during the consecutive levels) is 408.

If conventional VBEM [6] is employed, 16641 grid points are required to have the same grid spacing with the 8-th level of QVBEM. Fig. 3-b depicts the required number of grid points in QVBWM and full-grid VBEM, to have the same grid spacing. As can be seen, the number of required grid points in VBEM grows exponentially, and thus, it is impractical in real applications.

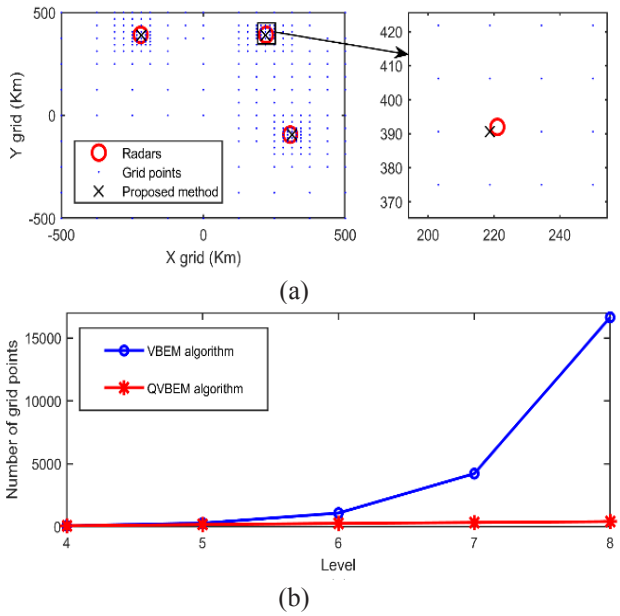

Fig. 3. (a) QVBEM localization after 8 levels. (b) Comparison of the number of grid points between QVBEM and VBEM with the same grid spacing.

Level	4	5	6	7
Full grid VBEM	0.44	6.33	243.16	10230
QVBEM	0.59	2.47	3.48	15.12

Table 1. Simulation run time for levels 4,5,6 and 7 (seconds).

Table 1. compares the simulation run time in QVBEM and full-grid VBEM. To compare the proposed method with other sparse recovery method, three methods are considered with the same number of grid points. We show the localization results of the StOMP [9], the VBEM [4] and the QVBEM, all using approximately the same number of grid points, in Fig. 4. The achieved localization errors are shown in Table 2. Note that the number of grid points in VBEM and StOMP is 289, while 232 grid points are used for QVBEM. As can be seen from Fig. 4 and Table 2, the QVBEM has considerably better accuracy with approximately the same number of grid points.

To study the trade-off between the threshold value and computational complexity, Fig. 5 simultaneously demonstrates the total number of grid points of QVBEM and the average localization error, in terms of threshold value.

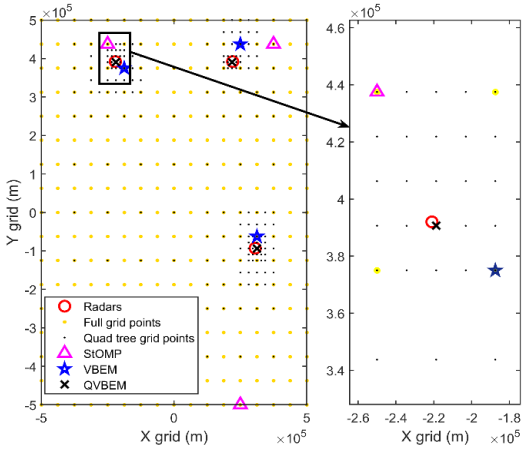

Fig. 4. Comparison between proposed QVBEM, conventional VBEM, and greedy StOMP algorithms.

Algorithm	Number of grid points	Mean error (m)	SNR (dB)
StOMP	289	208457	15
VBEM	289	40902	15
QVBEM	232	3938	15

Table 2. Average localization error.

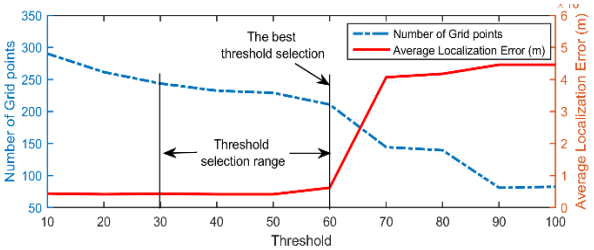

Fig. 5. Threshold selection range.

As expected, by increasing δ, the total number of grid points is decreased, and at the same time, the average localization error is increased. For the threshold values below 60, the localization error is approximately reach to its minimum, however, the lower threshold means the larger number of grid points. For the threshold values between 30 and 60, the number of grid points changes only slightly. Thus, any value in this range can be selected.

7. CONCLUSION

Accurate localization of ground-based radars, located in a wide geographical area, from a space-borne platform is a challenging problem. We have proposed to combine the well-known VBEM recovery algorithm with the Quad-tree technique to make a low-complexity and accurate sparse recovery method. The proposed QVBEM algorithm starts with low-density grid points and iteratively uses local grid-points refinement around the potential targets, with the aid of Quad-tree technique. Simulation results, show the considerably reduction in time and computational complexity. The trade-off between localization error and computational complexity is also investigated.

REFERENCES

[1] T. Yu, A. Haniz, K. Sano, R. Iwata, R. Kosaka, Y. Kuki, G.K. Tran, J.I. Takada, and K. Sakaguchi., "A guide of fingerprint based radio emitter localization using multiple sensors," IEICE IEICE Transactions on Communications, vol. E101-B, no. 10, pp. 2104-2119 Oct. 2018.

[2] E. Ramezani, M.F. Sabahi, and S.M. Saberali, "Joint frequency and two-dimensional direction of arrival estimation for electronic support systems based on sub-Nyquist sampling," IET Radar, Sonar & Navigation, vol. 12, no. 8, pp. 889-899 Apr. 2018.

[3] S. K. Sharma, E. Lagunas, S. Chatzinotas, and B. Ottersten, "Application of compressive sensing in cognitive radio communications: a survey," IEEE Communications. Survey & Tutorials, vol. 18, no. 3, Feb. 2016.

[4] D.G. Tzikas, A.C. Likas, and N.P. Galatsanos, "The variational approximation for Bayesian inference," IEEE Signal Process. Mag., 2008, 25, (6), pp. 131–146.

[5] M. Lundgren, L. Svensson, and L. Hammarstrand, L., "Variational Bayesian expectation maximization for radar map estimation,"IEEE Trans. Signal Process. 64, (6), pp. 1391–1404, 2015.

[6] B. Sun, Y. Guo, N. Li, and D. Fang, "Multiple target counting and localization using variational Bayesian EM algorithm in wireless sensor networks," IEEE J. Selected Areas Communications, vol. 65, no. 7, pp. 2985-2998, 2017.

[7] T. Marka, J. Reif, "Quad tree structures for image compression applications," Information Processing and Management 0306-4573/92, vol. 28, n0. 6, pp. 707-721, 1992.

[8] E. Ramezani, 'Compressed parameters estimation in the space borne electronic warfare receiver'. PhD thesis, University of Isfahan, 2019

[9] D.L. Donoho, Y. Tsaig, I. Drori, and J. Starck, "Sparse solution of underdetermined linear equations by stagewise orthogonal matching pursuit, submitted to," in IEEE Trans. on Information theory 2006.